JOURNAL OF MECHANICAL ENGINEERING AND SCIENCES
ISSN: 2289-4659 e-ISSN: 2231-8380
VOLUME 17, ISSUE 3, 2023, 9597 – 9615
DOI: https://doi.org/10.15282/jmes.17.3.2023.6.0760

UNIVERSITI MALAYSIA PAHANG AL-SULTAN ABDULLAH

RESEARCH ARTICLE

Numerical analysis of non-Fourier heat conduction dynamics in the composite layer

R. Yuvaraj*, D. Senthilkumar

Faculty of Mechanical Engineering, Sona College of Technology, Salem, Tamilnadu, 636005, India
Phone: +91-427-4099711

ABSTRACT - This paper presents the numerical analysis of non-Fourier heat conduction in thin composite layers under asymmetrical boundary conditions. In the thermal barriers such as steam and gas turbine blades, thin film coating are used to protect the blade from thermal damage. The coating on the blades are very short in length. Heat conduction across thin composite layer with short time is examined using a finite element approach. With this very small duration with the finite speed of the thermal wave, the Fourier mode of heat conduction is disappeared due to the infinite speed of the thermal wave assumption. Therefore, analyzing the non-Fourier heat conduction in thin layers is essential. The developed model is executed in Python using Newmark's scheme and the constant average acceleration method to predict the temperature variation and temperature contours. The present model is validated with an experimental and numerical solution with good agreement. Besides, the temperature distribution across the composite layer with the entire length of the substrate and the coating for different thermal conductivity values, thermal diffusivity, and relaxation time are examined. It is noted that when the dimensionless k<1, the temperature after collision increases at the interface and decreases for k>1. The temperature contours are plotted to show that for any composite layers subjected to heat flux with short time durations and short distances. The non-Fourier heat conduction model produces more realistic results than the classical Fourier conduction model across the composite layer. The temperature increases after the collision at time η>0.5 for k=0.1 and reduces when k=10. The thermal wave propagates faster in the substrate, increasing temperature after the first collision at the interface for τ=0.1 and decreasing in temperature after collision with slower propagation in the substrate for τ=10. The sub-collisions are found on the substrate side with an increase in temperature θ=4.4 against the applied temperature of θ=3 for a more considerable value of thermal diffusivity α=10.

ARTICLE HISTORY
Received : 05th Dec. 2022
Revised : 10th June 2023
Accepted : 21st Aug. 2023
Published : 28th Sept. 2023

KEYWORDS
Non-Fourier conduction
Finite element model
Composite layer
Thermal wave
Relaxation time

1.0 INTRODUCTION

In the recent field of engineering, thin-film coatings are essential for thermal-related areas like thermal barriers, laser heating, phase-change devices, boiler tubes, heat exchangers, etc. It is necessary to study heat conduction through a composite layer due to the disappearance of classical Fourier law, in which the heat propagates with the infinite speed of a heatwave. There is no lag in heat flow through metal, and immediate response is carried by the temperature gradient when it is subjected to the applied heat flux. In the actual case, the orders of magnitude of the time and space dimensions are tiny in thin layers coated on the substrate for different thermal applications. This minimal duration with finite speed of thermal wave offers a lag called relaxation time τ between the applied heat flux to the temperature gradient. This allows the non-Fourier mode of heat conduction across the layers, and the Fourier mode of heat conduction is disappeared due to the infinite speed of thermal wave assumption.

The non-Fourier heat conduction model produces considerably different results from those predicted by the Fourier model at very short time scales. Thus, a modified heat flux model for Fourier heat conduction law is important to account for phenomena involving the finite propagation speed of the heatwave. Cattaneo [1] and Vernotte [2] independently suggested a modified heat flux Cattaneo-Vernotte (CV) model in the form coupled with the local energy balance to eliminate the anomalies and infinite speed of thermal wave propagation. Maurer and Thompson [3] analytically investigated the non-Fourier effects in high heat flux conditions using the relaxation model for heat conduction and predicted the instantaneous jump in the surface temperature. Ozisik and Vick [4] studied the wave nature of thermal energy transport analytically. They found that the thermal wavefront travels through the finite slab containing a volumetric energy source at finite propagation speed, dissipating energy in its wake and reflecting from the surface. Goodson and Flik [5] examined that the size effect in films is of the greatest importance while the phonon conductivity dominates over the electron conductivity. When the heat transfer takes place in a very short time interval, the Fourier heat conduction model cannot predict the temperature distribution very accurately. Ozisik [6] and Tzou [7] analytically solved the simple thin-film heat conduction problem. Xu et al. [8] and Tan [9,10] presented the solutions for the hyperbolic heat conduction

***CORRESPONDING AUTHOR | R. Yuvaraj** | ✉ yuvarajr@sonatech.ac.in
© The Authors 2023. Published by Universiti Malaysia Pahang Publishing. This is an open access article under the CC BY-NC 4.0 license

equation across thin films. The wave propagation, temperature overshoot that occurred in the film, dissipation of thermal energy, and reflection of the thermal wave is analyzed for the abnormalities of the infinite speed of thermal wave across the thin film [11–14]. Lewandowska [15] presented an analytical solution of the hyperbolic heat conduction equation for the case of a thin slab symmetrically heated on both sides. The solution obtained by Laplace transforms the method taking advantage of the method of superposition. Peterson et al. [16] solved the non-homogeneous and time-dependent heat conduction boundary value problem within a two-dimensional rectangular slab using the integral-transform technique and presented the temperature distribution subjected to a time-varying and spatially decaying laser source. Lam and Fong [17] gave an analytical solution for heat diffusion vs. wave propagation in solids subjected to an exponentially-decaying heat source using the method of superposition and solution structure theorem. Thermal wave phenomena in a thin film subjected to the non-homogeneous boundary are solved analytically by Fong and Lam [18]. They used the superposition principle in conjunction with the solution structure theorems.

A few research works experimentally obtained the anomalies of the infinite speed of thermal waves, and their results clearly showed the finite speed of thermal waves across thin layers. Mitra et al. [19] presented experimental evidence of hyperbolic heat transfer in processed meat for different conditions and experimentally determined the relaxation time for processed meat. Kaminski [20] discussed the range of differences in the description of heat transfer by parabolic and hyperbolic heat conduction equations and proposed the relaxation time τ experimentally for different materials. Roetzel et al. [21] conducted a wide range of experiments, revealing a definite hyperbolic effect in the "bulk" conduction behavior of materials with a non-homogeneous inner structure. Hence, it is very important to consider the non-Fourier effect of heat conduction in thin layers. Plenty of numerical works also presented evidence for the hyperbolic heat conduction model. They analyzed the importance of the relaxation time, reducing the immediate response between the heat flux and the temperature gradient. Koay et al. [22] presented a method for reverse-time transmission line matrix (TLM) modeling of thermal diffusion problems described by the hyperbolic heat conduction equation and investigated the reverse time algorithm numerically. Torii and Yang [23] studied numerically the effect of laser radiation on the propagation phenomenon of a thermal wave in a very thin film subjected to symmetrical heating on both sides using the explicit scheme, MacCormack's predictor-corrector scheme. They found that the temperature overshoot in a very thin film within a very short time.

Lor and Chu [24] numerically examined the superconductor film depositions on several commonly used substrates. They used a finite difference method to solve the hyperbolic heat conduction problem in the film and substrate composites under an imposed surface heat flux on the exterior film surface. They found that the reflection and transmission occur at the contact surface of the dissimilar material that depends on the substrate properties and interface conditions. Also, the hyperbolic equation predicts significantly different results from those indicated by the parabolic equation at small time scales. Also, Lor and Chu [25] extended their work to analyze the effect of interface resistance in heat transfer across two-layered composite media under an incident pulse energy exerting on the exterior surface of one layer by using the hyperbolic heat conduction equation. Chen and Liu [26] analyzed the hyperbolic heat conduction problem in the film and substrate composite under a pulsed volumetric source adjacent to the exterior film surface using the hybrid application of the Laplace transform technique and the control-volume method in conjunction with the hyperbolic shape functions. Li et al. [27] developed numerical methods for transient heat conduction in multilayer materials using an implicit difference scheme to analyze the stability of the hyperbolic equation. The results are compared with the numerical results from the parabolic heat conduction equation. The results illustrate the time scale required for metal films to establish equilibrium in energy transport, which makes it possible to determine a priori the time response and the measurement accuracy of the metal film. Hyperbolic heat conduction equations in a thermal barrier coating structure under an imposed heat flux on the exterior of the coating are solved numerically by Akwaboa et al. [28] using the mean value finite volume method. In all the previous works, the complete thermal wave propagation from transient to steady-state conditions and temperature variation through the full length of the thin layer as well as the substrate across the composite layer has not been presented yet. Recently, Yuvaraj and Senthil Kumar [29] presented numerically complete thermal wave propagation and collision across the thin layer from transient to steady-state using the finite element approach has been studied. Also, temperature contours, the transition of parabolic to hyperbolic nature, and temperature variation near the surface are plotted by considering the hyperbolic mode of heat conduction. Mozafarifard et al. [30] investigated heat transfer in thin metal films subjected to a short-pulse laser and observed the non-Fourier phenomenon in the temperature response of thin metal films due to the short temporal scales and high intensity of laser pulses during the heating process. Liu et al. [31] analyzed the effects of relaxation time, shape, and the frequency of the base temperature oscillations on heat transfer efficiency by using Lattice Boltzmann Method to solve the non-Fourier heat conduction in a fin under periodic boundary conditions. Dong et al. [32] presented an analogy analysis between non-Fourier heat conduction and non-Newtonian momentum transport and derived a new governing equation for momentum transport in nanosystems, which predicts the varying effective viscosity in a steady flow. Khosravirad and Ayani [33] developed a bioheat transfer model that includes the effects of metabolic heat generation, capillary blood vessels, and relaxation times of heat flux and temperature gradient to study the non-Fourier heat conduction behavior in spherical breast tumors during the laser hyperthermia process. Hu et al. [34] investigated the thermal shock fracture problem of the auxetic honeycomb layer based on non-Fourier heat conduction. The uncracked non-Fourier temperature and thermal stress field are determined by the separation of variables method and the constitutive model of the auxetic honeycomb layer.

In the present work, a finite element model is developed to predict the propagation and collision of the heatwave in composite layers subjected to asymmetrical boundary conditions. The current model is applicable for any kind of composite layer of two materials with one interface. The second-order non-Fourier heat conduction equation is solved numerically by considering the Cattaneo-Vernotte heatwave model. Physically, it means that there is a time lag between heat flux and temperature gradient. The effects of temperature changes in the time and space increments on a thin layer are discussed. Newmark's scheme is used to solve the finite element hyperbolic heat transfer model. The present finite element model is validated with the experimental solution presented by Mitra et al. [19] and the numerical solution given by Lor and Chu [24] of similar configuration and conditions with good agreement. The complete heat wave propagation and collision of a heatwave at the interface of the composite layer and the total length of the substrate are examined, and the propagation of heatwaves in different layers is compared by varying thermal conductivity k, relaxation time τ and thermal diffusivity α. Besides, temperature contours are plotted across the composite layer for the full length of the coating and substrate. The present model provides the solution for heat conduction across the composite layer used in thermal barriers, laser heating, phase-change devices, boiler tubes, heat exchangers, condensers, turbine blades, etc.

2.0 PROBLEM DESCRIPTION

A composite layer contains two-layer is shown in Figure 1. The first layer shows the thin layer of length L_1, and the second layer shows the substrate of length L_2. Assumes one-dimensional heat conduction across the thin layer without heat generation, with thermal conductivity k, density ρ, and specific heat capacity c_p, respectively. It is subjected to a constant temperature at the left boundary and insulation at the right side boundary. The entire layer is initially maintained at dimensionless temperature of 1. The left and right side boundaries are suddenly changed and maintained at a dimensionless temperature of $T_{w1} = 3$. Due to the temperature difference between both boundaries and the initial temperature of the layer, heat transfer occurs, and the heatwave propagates at a finite speed across the layer.

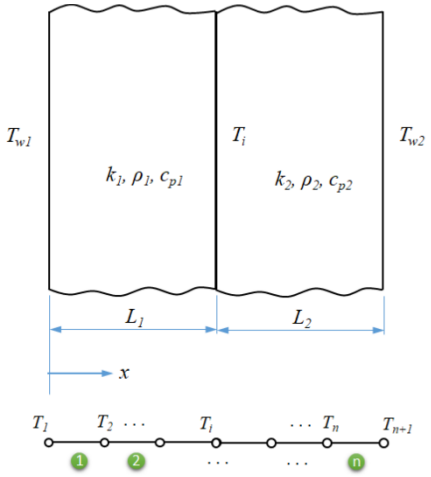

Figure 1. Composite layer

The mechanism of heatwave propagation in a thin layer is entirely different from the classical model of Fourier heat conduction. The temperature at all points throughout the layer is predicted to analyze the mode of heatwave propagation in a thin layer by solving the hyperbolic heat conduction equation using a finite element dimensionless approach.

3.0 MODELING AND SIMULATION

The governing equations are solved for the simulation of thermal wave propagation at the composite layer interface, including the classical Fourier heat conduction equation, CV-modified conduction equation, and local energy balance equation. The Fourier heat conduction equation is given as,

$$q = -k\,\nabla T \tag{1}$$

where q is the heat flux, k is the thermal conductivity, and ∇T is the temperature gradient. When the body is subjected to the boundary condition or initial condition instantly, the speed of heat propagation in the body is always finite. Thus, a more precise heat flux model must be assumed to modify the Fourier heat conduction law to account for phenomena involving the finite propagation speed of the heatwave. Cattaneo [1] and Vernotte [2] independently suggested a modified heat flux model in the form coupled with the local energy balance as,

$$\tau\frac{\partial q}{\partial t} + q = -k\,\nabla T \tag{2}$$

where, τ is the relaxation time, the effect of relaxation time is essential in a thin layer or short-duration heating when it becomes zero, the Eq. (2) is reduced to the classical Fourier conduction equation. The energy equation for anisotropic material can be written as,

$$\nabla q = -\rho c_p \frac{\partial T}{\partial t} \tag{3}$$

where, ρ is the density and cp is the specific heat capacity. The given governing equations are in the form of dimensional characters that are converted into non-dimensional form by using the following dimensionless parameters,

$$\xi = \frac{\mathrm{cx}}{2\alpha}, \eta = \frac{\mathrm{c^2 t}}{2\alpha}, \theta = \frac{\rho \mathrm{c^2 T}}{\mathrm{q_r}}, \zeta = \frac{\mathrm{q}}{\mathrm{q_r}}, \tau = \frac{\alpha}{\mathrm{c^2}}, k = \frac{k_2}{k_j} \tag{4}$$

where, ξ is the dimensionless distance in x direction with thermal wave speed c in solids, η is the dimensionless time, θ is the dimensionless temperature, and ζ is the dimensionless heat flux. kj is the dimensionless thermal conductivity with j=1, and 2 represents the thin layer and substrate, respectively. The Eq. (4) provides the propagation of theraml wave across the composite layer with same value of dimensionless time η and length ξ similarly used in the work presented by Lor and Chu [24].

The energy and CV equations are expressed in the dimensionless parameters given in Eq. (4) can be written as

$$\frac{\partial \mathrm{T_j}}{\partial t} + \frac{1}{k_j}\frac{1}{\alpha_j}\frac{\partial \mathrm{q_j}}{\partial x} = 0 \tag{5}$$

$$\frac{\partial \mathrm{q_j}}{\partial t} + \frac{k_j}{\tau_j}\frac{\partial \mathrm{T_j}}{\partial x} = -2\frac{1}{\tau_j}\, q_j \tag{6}$$

Initial conditions:

$$\theta(\xi, \eta) = 1 \quad at\ \eta = 0, \quad 0 < \xi < 1 \tag{7}$$

$$\frac{\partial \theta}{\partial \eta}(\xi, \eta) = 0 \quad at\ \eta > 0, \quad \xi = 0, \quad \xi = 1 \tag{8}$$

Boundary conditions:

$$\theta(\xi, \eta) = 3 \quad at\ \xi = 0, \quad \eta > 0 \tag{9}$$

$$\frac{\partial \theta}{\partial \eta}(\xi, \eta) = 0 \quad at\ \xi = 1, \quad \eta > 0 \tag{10}$$

$$\theta(\xi, \eta) = 2 \quad at\ \xi = 30.5, \quad \eta > 0 \tag{11}$$

The finite element method discretizes the given domain into several subdomains called finite elements. The approximation functions of weighted residuals are constructed on each element to solve the problem. The procedure to develop a finite element model is given by Reddy [35].

The one-dimensional finite element model for the composite layer, from Eq. (5) and Eq. (6) can be written as

$$\frac{\partial \mathrm{U_j}}{\partial t} + [A]_j \frac{\partial \mathrm{U_j}}{\partial x} = S_j \tag{12}$$

where, $U_j = \begin{Bmatrix} T_j \\ q_j \end{Bmatrix}$, $S_j = \begin{Bmatrix} 0 \\ -2\frac{1}{\tau_j}\, q_j \end{Bmatrix}$, $[A]_j$ is the Jacobian matrices.

$$[A]_j = [R]_j [\lambda]_j [R]_j^{-1} \tag{13}$$

where, k denotes the diagonal matrices consisting of two eigenvalues of $[A]$ for each layer. The superscript -1 represents the inverse eigenmatrix. The diagonal matrices and the right eigenmatrices show that

$$[\lambda]_j = \begin{bmatrix} -\left(\frac{\alpha_j}{\tau_j}\right)^{1/2} & 0 \\ 0 & \left(\frac{\alpha_j}{\tau_j}\right)^{1/2} \end{bmatrix} \tag{14}$$

$$[R]_j = \begin{bmatrix} 1 & 1 \\ -k_j \left(\frac{1}{\alpha_j\, \tau_j}\right)^{1/2} & k_j \left(\frac{1}{\alpha_j\, \tau_j}\right)^{1/2} \end{bmatrix} \tag{15}$$

Then Eq. (5) contains the temperature gradient concerning time and the heat flux gradient with space. Whereas, in Eq. (6) contains the opposite temperature gradient and heat flux gradient, forming the form of coupled equations. The coupled equations are rearranged as a single variable equation, Eq. (12), and now it can be solved using the finite element approach given by Yuvaraj and Senthil Kumar [29].

4.0 COMPUTATIONAL ALGORITHM

The present work anaysis the temperature variation across the composite layer by solving the Eqs. (5) and (6) subjected to the initial and boundary conditions given in the Eqs. (7) to (11). The computational algorithm to find the temperature across the composite layer is shown in the form of flow chart given in the Figure 2. In the present work, finite element method is used for solving hyperbolic equation and it is important to choose the number of elements n. The procedure the choose the number of elements is discussed in the Mesh sensitivity test chapter. It is also very important to find the step size $\Delta\eta$ for the computation to achieve the solution convergence for the hyperbolic equation.This step size is empirically choosed as $\Delta\eta = 1 \times 10^{-4}$ in the present work.

The model is coded in Python and executed using Python 3.6.3 version open source software. The following computational procedure is followed to obtain the finite element hyperbolic heat conduction solution in a thin layer.

i) Select the number of elements n and dimensionless time step $\Delta\eta$ and dimensionless length of the layer ξ.

ii) Discretize the film's length ξ into n number of elements in array form by importing the *NumPy* module.

iii) Set the initial conditions and boundary conditions given in Eqs. (7) to (11).

iv) Develop the code for stiffness matrix $[K]$, capacitance matrix $[C]$, and mass matrix $[M]$ in the form of a matrix using the *NumPy* module (Yuvaraj and Senthil Kumar [29]).

v) Solve the Eqs. (5) to (6) for hyperbolic mode

   a. First, find the value of $[A]j$ as given by Lor and Chu [24]

   b. Find the value of Sj from the known values of q_j and τ

   c. Apply the value of $[A]_j$ and S_j in Eq. (12) and find the value of U_j

   d. Apply the values of U_j and find the value of T_j

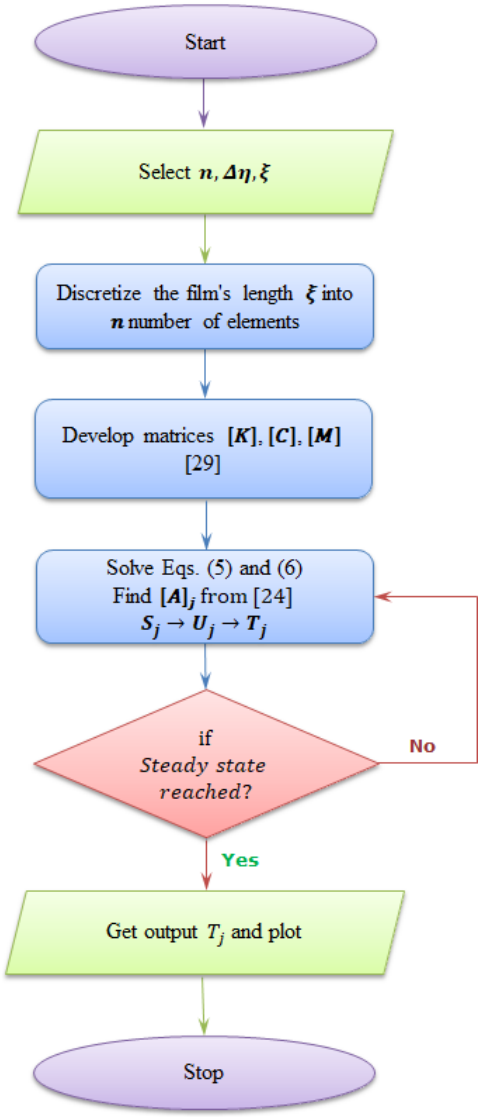

Figure 2. Flow chart for computation

5.0 RESULTS AND DISCUSSION

5.1 Mesh Sensitivity Test

The given thin layer L_1 is tiny compared to substrate length L_2. In the present work, the substrate length L_2 is 60 times greater than the coating layer thickness L_1 as, similar to the condition used by Lor and Chu [24]. The mesh sensitivity test is examined for the number of elements n varying from 400−2500, and the results are shown in Figure 3. The time difference of 10^{-4} is used to solve the present finite element model. From Figure 3, it is noted that an increasing number of elements from n=2200 to n=2500 make no effects and produce similar results. Hence, the number of elements is taken as n=2200 for the present work. The composite layer thickness L is discretized into 2200 finite elements, and the interface nodal temperature between consecutive nodal points is determined by applying the boundary conditions and initial conditions given in Eqn. (7-11). The accuracy of the present model is similar to the numerical solution provided by Lor and Chu [24] at the interface of the layer and the substrate, as shown in Figure 3. Initially, the temperature is assumed as θ=1 throughout the layer thickness ξ. At time η>0, the left and right sides are suddenly changed to θ=3 at ξ=0 and ξ=1, respectively. The temperature at both boundaries is kept constant, and the temperature gradient at the boundaries $\frac{\partial \theta}{\partial \eta} = 0$ for the time η>0.

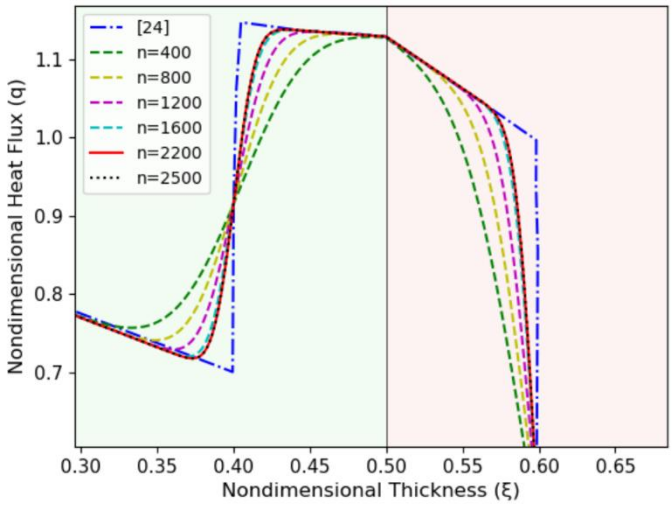

Figure 3. Mess sensitivity test

5.2 Validation of Present Work

The developed finite element model is validated with the numerical solution presented by Lor and Chu [24]. In their study, a similar boundary condition of asymmetrical boundary condition was used between the layer side and substrate side. The dimensionless heat flux of $q = 1$ was applied to the boundary of the layer, and the dimensionless thickness $\xi = 0.5$ was taken as layer thickness. On the substrate side, dimensionless thickness $\xi = 0.5$ was used to simulate the thermal wave propagation across the interface of the layer and the substrate as shown in Figure 4. The present finite element model is validated with the numerical solution presented by Lor and Chu [24] with the similar boundary condition. The thermal wave propagation from the left of the layer boundary towards the interface of the layer and the substrate is simulated by using the Newmark scheme. The results are plotted for the dimensionless duration of $\eta = 0.2, 0.4\ and\ 0.4$ are shown in Figure 4. When the thermal wave propagates across the interface of the layer and the substrate, it propagates with a different pattern for different dimensionless thermal conductivity $k = 0.1, 1\ and\ 10$. If the layer side thermal conductivity is lower than the substrate side, there is a sudden drop in heat flux across the interface. If the layer side thermal conductivity is greater than the substrate side, there is a sudden rise in temperature across the interface. Whereas, for similar thermal conductivity on both sides, there is a smooth propagation of thermal occurs as shown in Figure 4. The validation made a good agreement as shown in Figure 4. The deviation shows the discretization error caused by the finite element method. The complete heat wave propagation and collision of a heatwave at the interface of the composite layer are examined until it reaches a steady state.

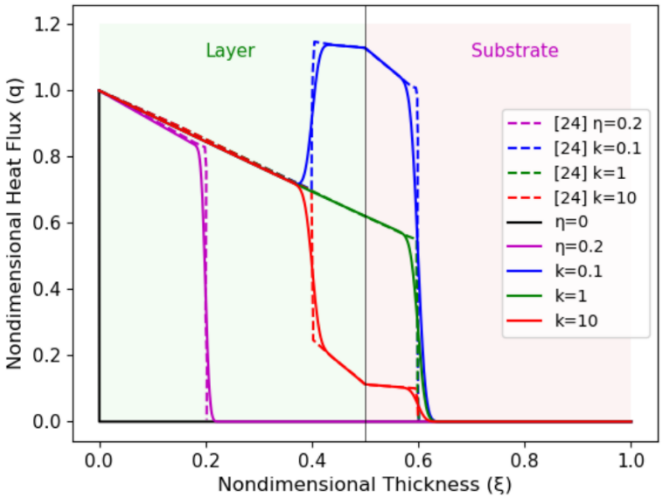

Figure 4. Validation of the present non-Fourier model across the composite layer with the numerical solution given by Lor and Chu [24]

The finite element model for hyperbolic heat conduction is also compared with the three experimental results, two from *Experiment-1* and one from *Experiment-4*, of Mitra et al. [19], as shown in Figure 5. The non-dimensional temperature and time are plotted in Figure 5(a) for the heat conduction that occurred within the processed meat when the thermocouple in the Room sample was placed at 6.3 mm from the interface against the *Experiment-1* conditions. It shows the evidence for the hyperbolic nature of heat transfer across the meat with a sudden jump in the temperature of the meat at the point 6.3 mm from the interface at dimensionless time of 4.2. Figure 5(b) depicts the temperature variation of the thermocouple in the processed meat when the thermocouple is placed at a distance of 6.6 mm from the interface. The hyperbolic temperature jump occurs at dimensionless time of 4.7. It is lower than that of the aforementioned case at a distance of 6.3 mm. The hyperbolic nature of temperature jump is continuously vanished with increasing the position of the thermocouple.

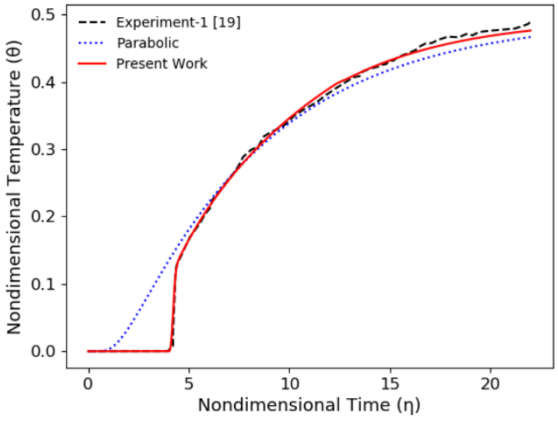

(a)

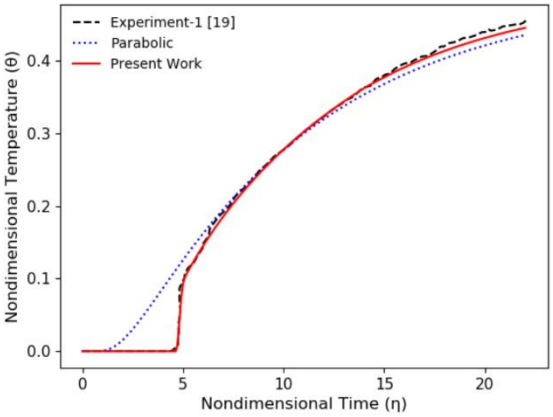

(b)

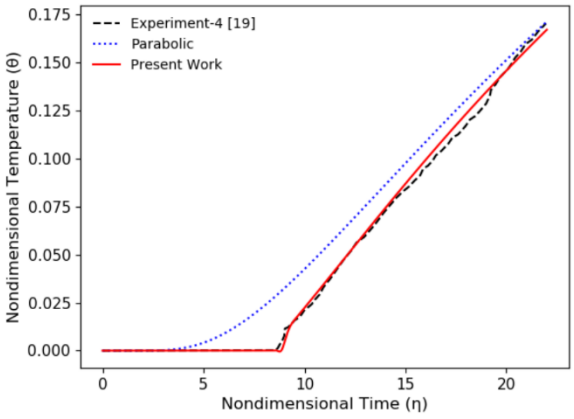

(c)

Figure 5. Validation of the present non-Fourier model across the composite layer with the experimental solution given by Mitra et al. [19]

Figure 5(c) is plotted with the temperature variation obtained from the thermocouples placed at 14 mm from the interface for the *Experiment-4* conditions. The numerically predicted results are compared with the experimental results, and Figure 5 shows that the present results are closely related to the experiment, Experiment-1, and Experiment-4, Mitra et al. [19].

5.3 Thermal Wave Propagation and Collision for Different Thermal Conductivity

The non-dimensional terms kj, τj, and αj are referenced as k, τ, and α respectively, from this point forward. The non-dimensional thermal conductivity k=$k2k1$, refers to the ratio of thermal conductivity of the substrate to the thin film coating. The non-dimensional thermal conductivity k=1, means that both layers contain similar thermal conductivity. The thermal wave propagation across the composite layer is analyzed by taking the value of k as k=0.1, k=1, and k=10.

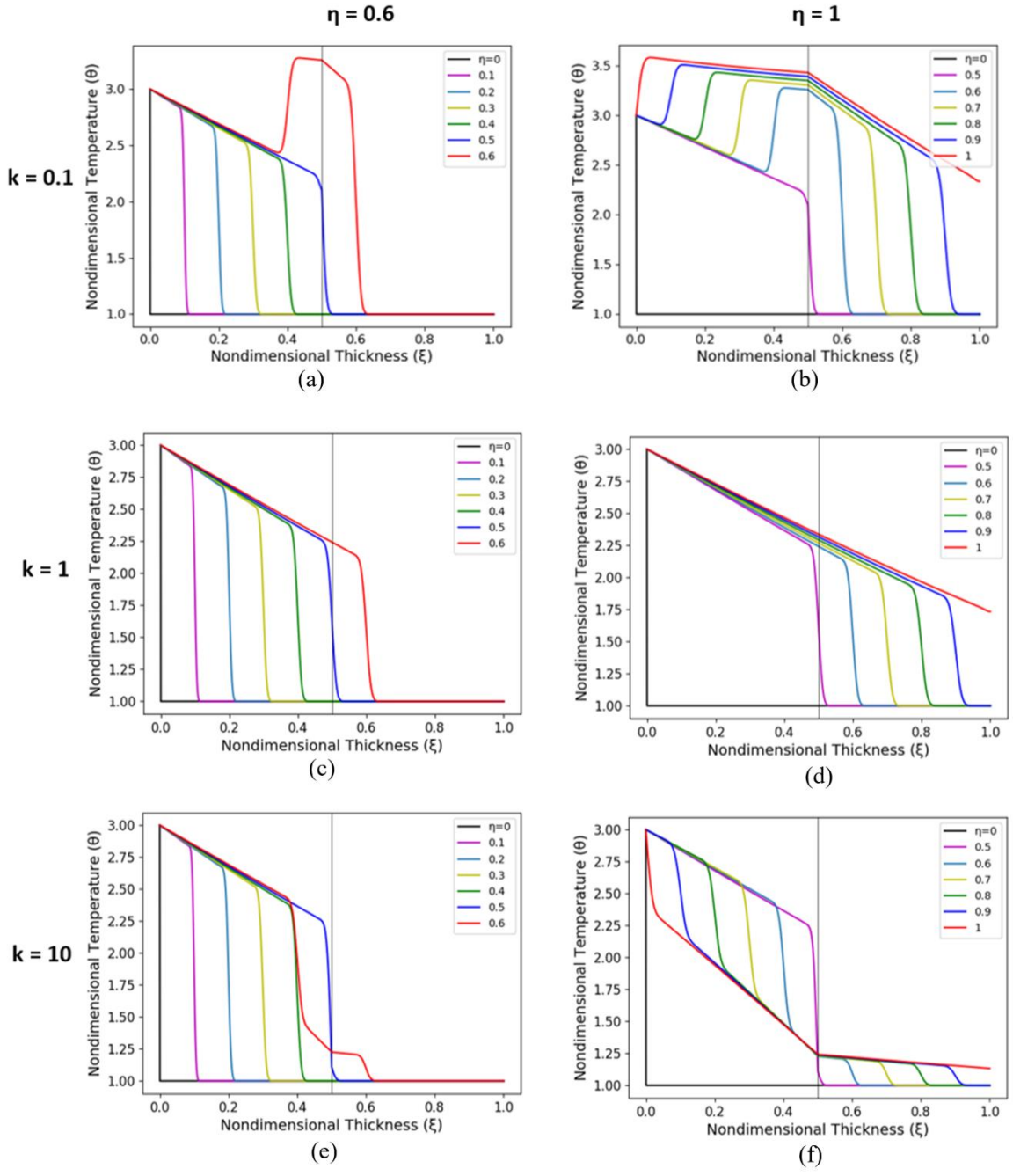

Figure 6. Thermal wave propagation across composite layer from η=0 to η=1 for different thermal conductivities, (a-b) k=0.1, (c-d) k=1 and (e-f) k=10

The dimensionless thermal conductivity k=0.1, higher coating layer thermal conductivity compared with the substrate, is considered to solve the given finite element model to predict the presence of thermal wave in a composite layer, propagation of the thermal wave, and collision behavior of thermal waves with advancing and reverse propagation. The thermal waves collide precisely at the interface of the composite layers, and the thermal wave propagation wave from time η=0 to 1 is shown in Figure 6. The thermal wave propagates from the boundary towards the interface from η=0.1 to

0.5 without any disturbances. When the thermal wave reaches the interface of the composite layer at ξ=0.5 and η=0.5. The first collision of the thermal wave occurs at the interface, and the amplitude of the wave is immense,s as shown in Figure 6(a) at η=0.6 after the collision and gives reverse wave towards the left boundary and forward propagation towards the right boundary. The temperature of the coating layer increases to θ=3.5, which is greater than the applied temperature of θ=3, as shown in Figure 6(b).

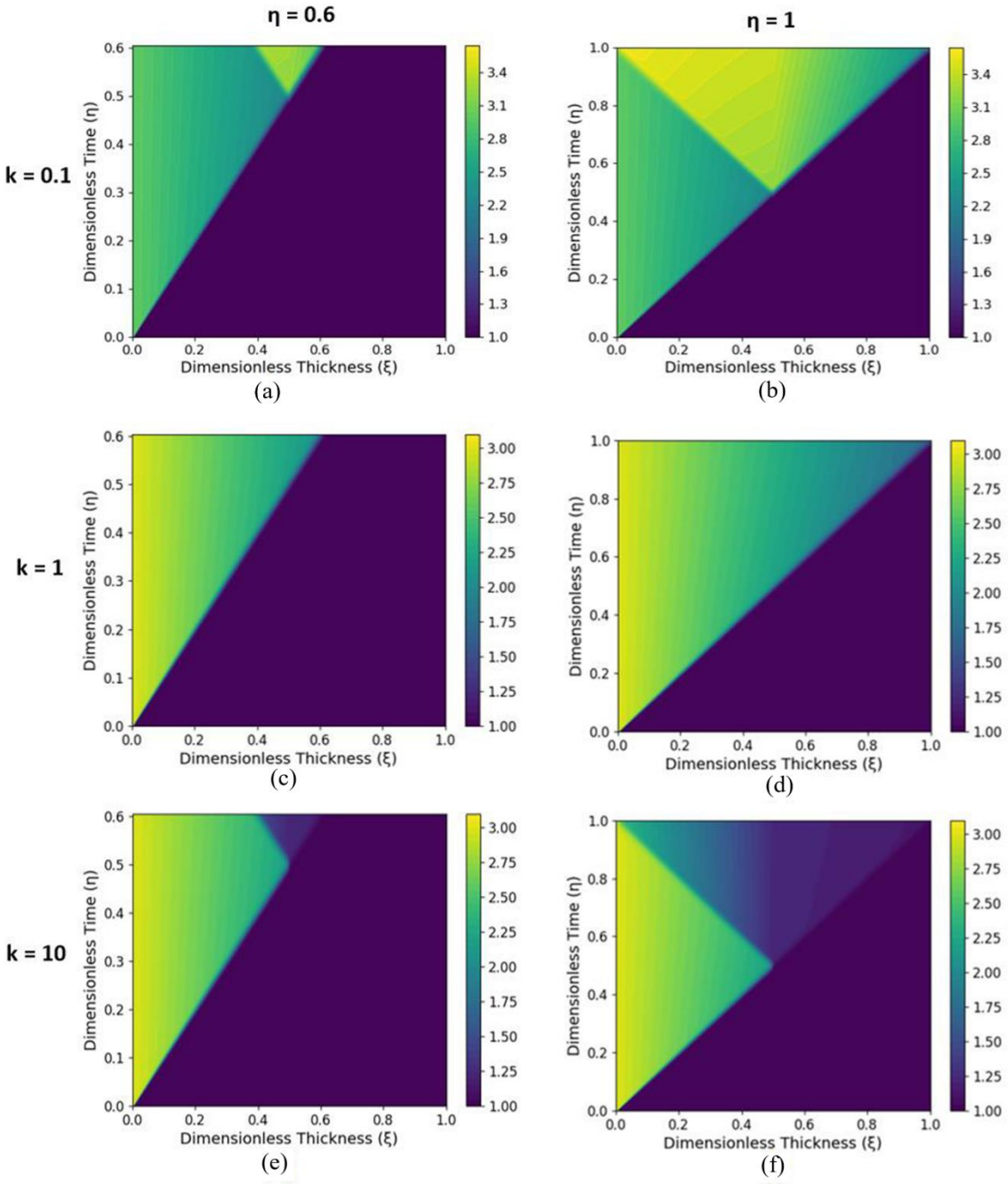

Figure 7. Temperature contours across composite layer from η=0 to η=1 for different thermal conductivities k=0.1, k=1, and k=10

Whereas in k=1 condition, Figure 7(c) and (d), there is no collision occurring at the interface, and the thermal wave propagates smoothly towards the right boundary. In the third condition, k=10, the thermal conductivity of the coating is lower than the substrate. The thermal wave propagation and collision are shown in Figure 7(e) and (f). The temperature of the composite layer decreases after the first collision, as shown in Figure 7(e), at η=0.6 due to the higher ability of the substrate to conduct heat than the coating. After the collision, the thermal wave propagates on either side of the boundary with a decrease in temperature.

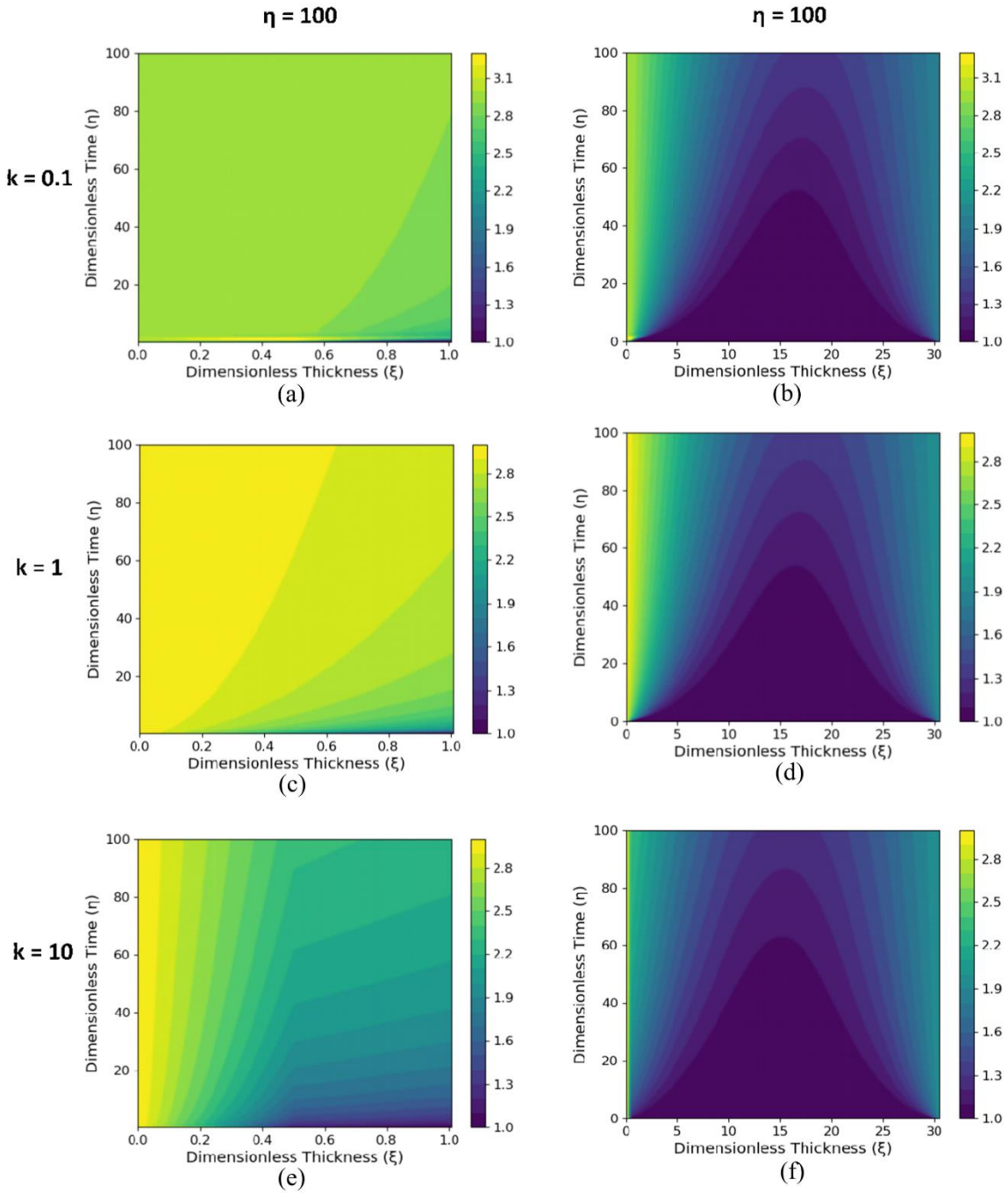

Figure 8. Temperature contours across the composite layer, for ξ=1 and the entire length of the substrate ξ=30.5, at η=100 for different thermal conductivities k=0.1, k=1 and k=10

The temperature contours across the composite layer from η=0−1 are plotted and shown in Figure 8. The high-temperature zone that occurs after the collision from η=0.5 onward is demonstrated in Figure 8(a). The reverse propagation of the thermal wave occurred after η=0.5 towards the left boundary, with the high-temperature zone remaining on the coating side for k=0.1. After the first collision, the sharp corner produced in the temperature contours represents thermal wave collision. Figure 8(c) and (d) shows the smooth propagation of thermal waves without any collision occurring for the condition k=1. The temperature distributed smoothly without sharp corners is evident in the absence of collision with k=1. Whereas, Figure 8(e) and (f) show the sharp corners with low-temperature profiles after the collision at η=0.5 due to the low thermal conductivity of the coating layer offering more thermal resistance to heat flow.

In addition, the temperature contours across the composite layer, for ξ=1 and the entire length of the substrate ξ=30.5, for η=100 with different thermal conductivities k=0.1, k=1 and k=10 are shown in Figure 8. The Fourier model heat conduction in macro size layers follows the parabolic nature of thermal waves without any wavefront, as shown in Fig. 7 (b), (d) and (e). The variation in temperature at the thin coating and the high-temperature zone occurs near the boundary when k=10, throughout the layer when k=0.1, and dissipates through the layers when k=0.1.

5.4 Thermal Wave Propagation and Collision for Different Relaxation Times

The non-dimensional relaxation time $\tau = \frac{\tau_2}{\tau_1}$, refers to the substrate's relaxation time ratio to the coating's relaxation time. The non-dimensional relaxation time τ=1, which means that both layers contain similar relaxation time. The thermal wave propagation and collisions across the composite layer are analyzed by taking the value of τ as τ=0.1, τ=1, and τ=10. The dimensionless relaxation time τ=0.1, lower relaxation time in the substrate than the coating is considered, and the thermal wave propagation and collision from time η=0 to 1 is shown in Figure 9.

In Figure 9(a), at η=0.6 the thermal wave moves faster than the other conditions when τ=0.1 and τ=10 due to the lower relaxation time, the immediate response of temperature gradient for the given applied heat of the substrate. The first collision of the thermal wave occurs at the interface, and the amplitude of the wave is slight raises, as shown in Figure 9(a) at η=0.6. After the collision, the thermal wave propagation towards the substrate side is faster than the reverse propagation towards the left boundary.

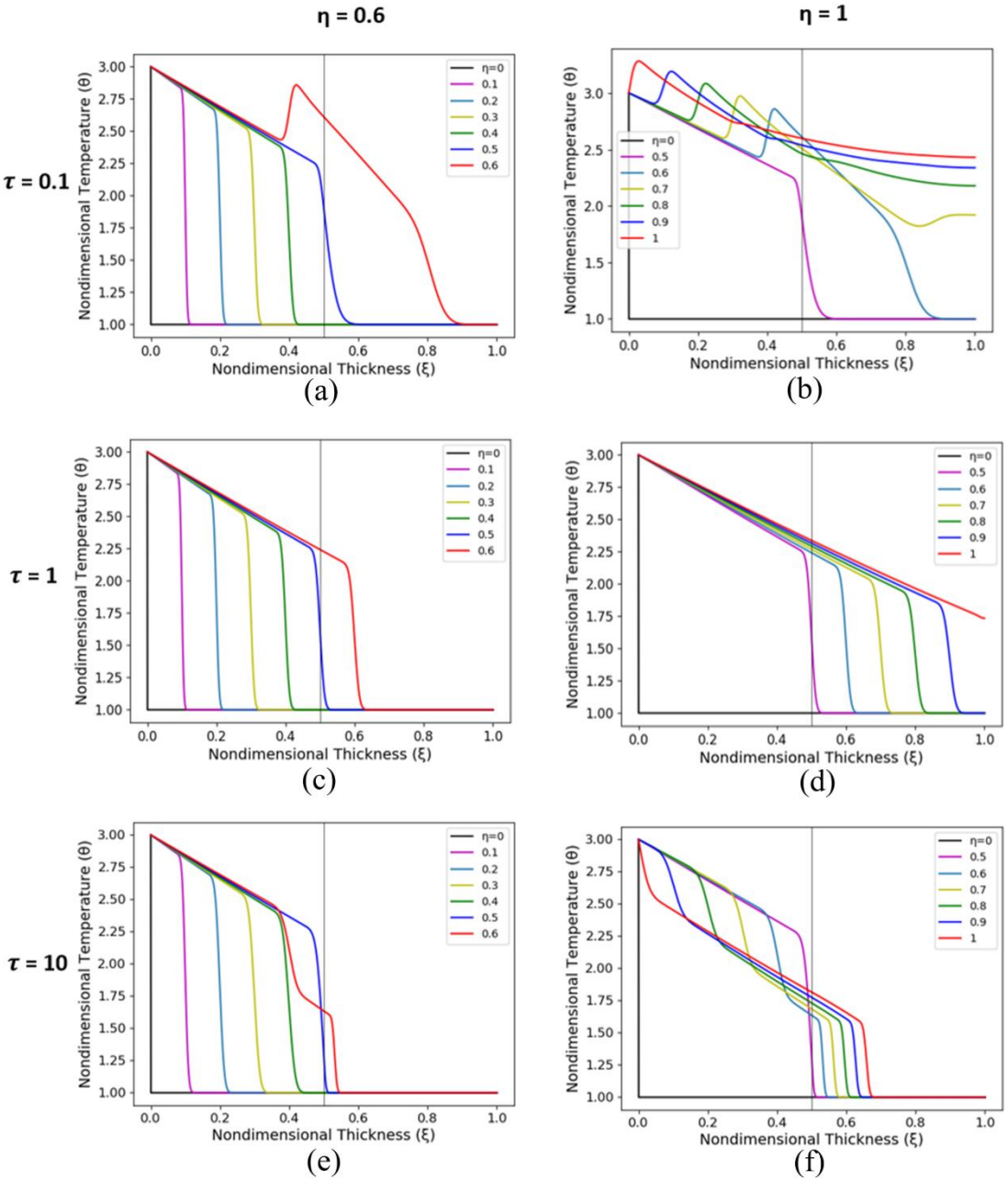

Figure 9. Thermal wave propagation across composite layer from η=0 to η=1 for different relaxation times, (a-b) τ=0.1, (c-d) τ=1, and (e-f) τ=10

Whereas k=10, the relaxation time of the substrate is higher than the coating, and the thermal wave propagates slowly due to poor response between the applied heat to the temperature gradient, as shown in Figure 10(e) after the collision. The temperature of the composite layer decreases after the first collision and propagates faster on the coating side and slower on the substrate side, as shown in Figure 10(f).

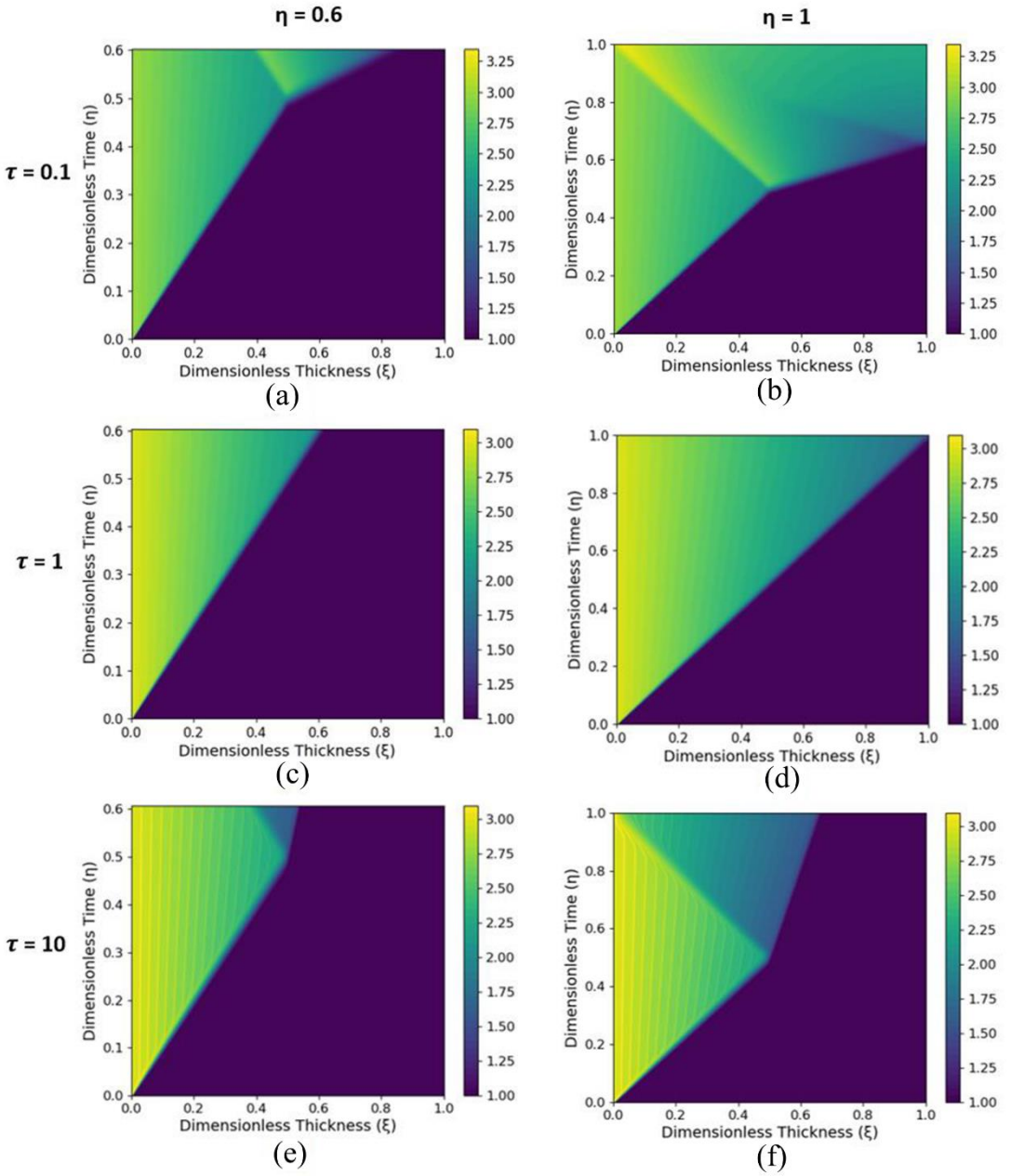

Figure 10. Temperature contours across composite layer from η=0 to η=1 for different relaxation times τ=0.1, τ=1, and τ=10

The temperature contours across the composite layer from η=0−1 are plotted and shown in Figure 10. The slight increase in temperature occurs after the collision from η=0.5 onward, which is shown in Figure 10(a). The reverse propagation of the thermal wave occurred after η=0.5 towards the left boundary, with a high-temperature zone remaining on the coating side for τ=0.1. The thermal wave takes time $\eta\approx$0.7 to reach the right side at ξ=1 for τ=0.1, whereas even at time η=1, the thermal wavefront just arrived ξ=0.7 due to the high relaxation time in the substrate as shown in Figure 10(f).

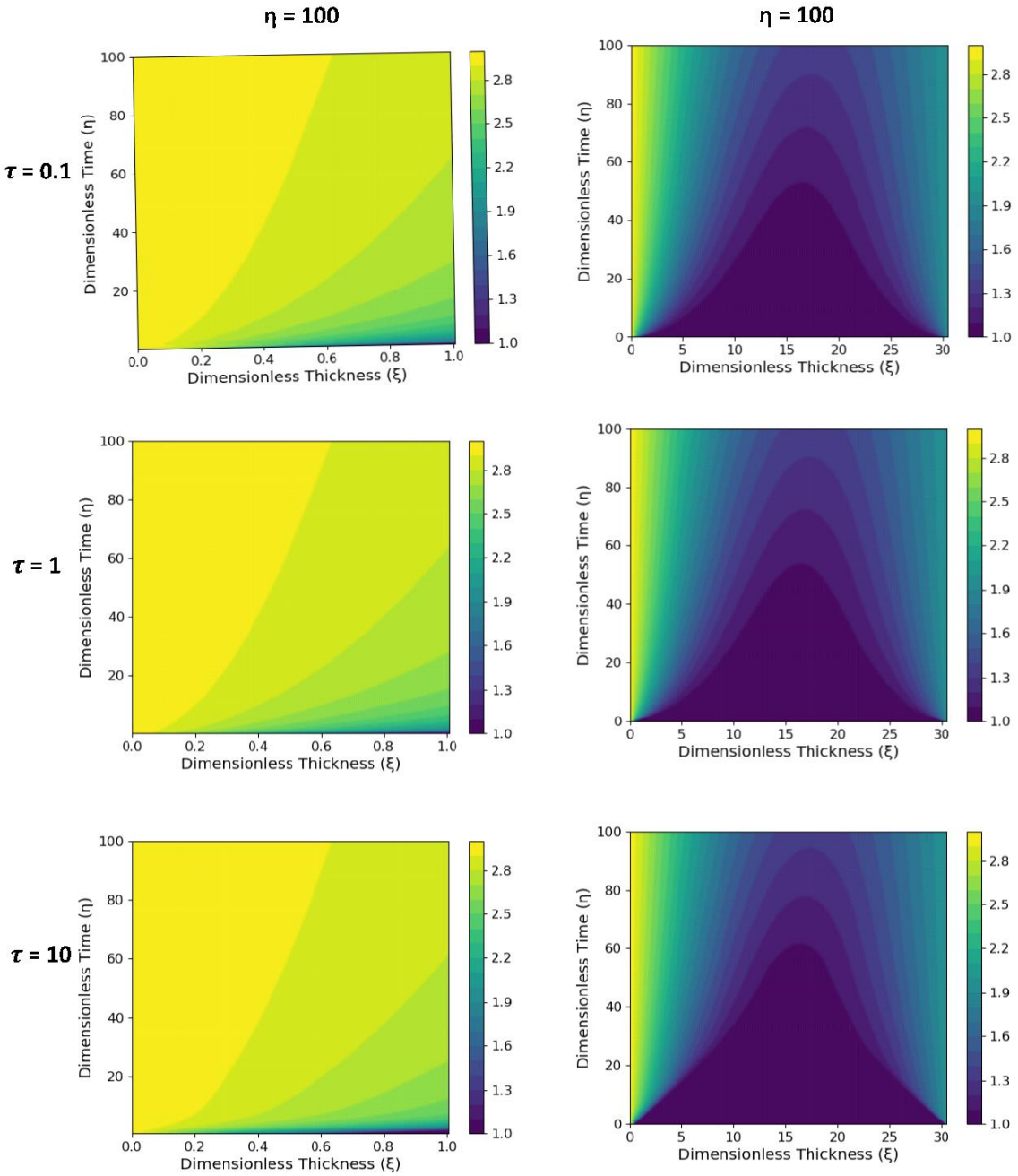

Figure 11. Temperature contours across the composite layer, for ξ=1 and the entire length of the substrate ξ=30.5, at η=100 for different relaxation time τ=0.1, τ=1 and τ=10

Also, the temperature contours across the composite layer, for ξ=1 and the full length of the substrate ξ =30.5, are plotted as shown in Figure 11. The time up to η =100 with different relaxation times τ =0.1, τ =1, and τ =10 are shown in Figure 11. It is noted that the change in relaxation time is not affecting the temperature when the distance and time are at the macro level. Relaxation time is significant when the distance and time are very short.

5.5 Thermal Wave Propagation and Collision for Different Thermal Diffusivity

The non-dimensional thermal diffusivity $\alpha = \alpha_2/\alpha_1$, is the ratio of the substrate's thermal diffusivity to the coating's thermal diffusivity. The thermal wave propagation and collisions across the composite layer are analyzed by taking the value of α as α=0.1, α=1 and α=10 as shown in Figure 12. The thermal wave propagates slowly for thermal diffusivity α=0.1, as shown in Figure 12(a) and (b), due to lower thermal diffusivity in the substrate than in the coating. After the collision, the temperature and propagation speed decreases on the substrate side than the reverse propagation on the coating side. There is a smooth thermal wave propagation that occurs for the condition α=1 without any collision, as shown in Figue 11(c) and (d).

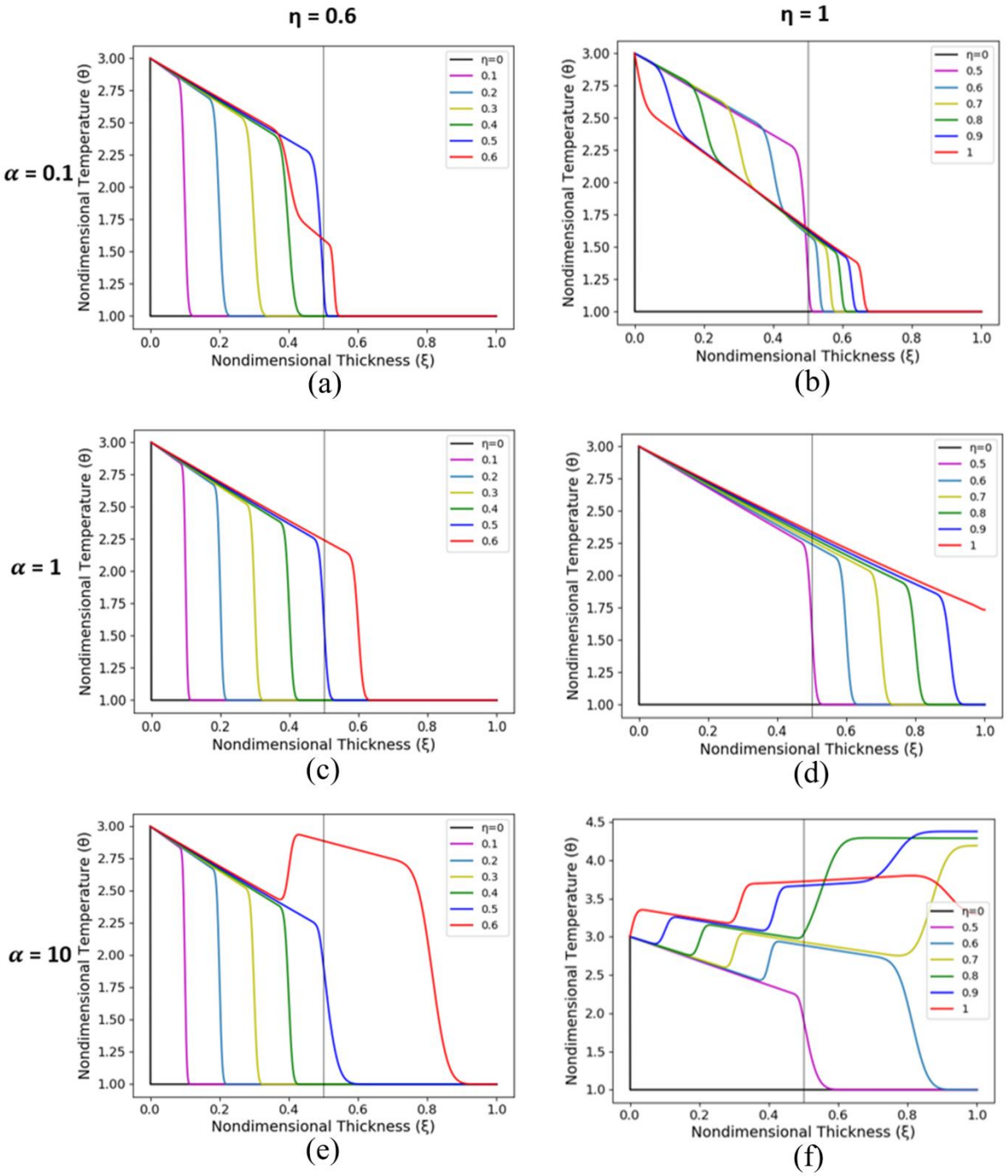

Figure 12. Thermal wave propagation across composite layer from η=0 to η=1 for different thermal diffusivity, (a-b) α=0.1, (c-d) α=1, and (e-f) α=10

Whereas α=10, the thermal diffusivity of the substrate is higher than the coating, the thermal wave propagates faster in the substrate than the coating side after the collision. The temperature of the composite layer increases after the first collision and propagates faster on the substrate side and slower on the coating side, as shown in Figure 12.

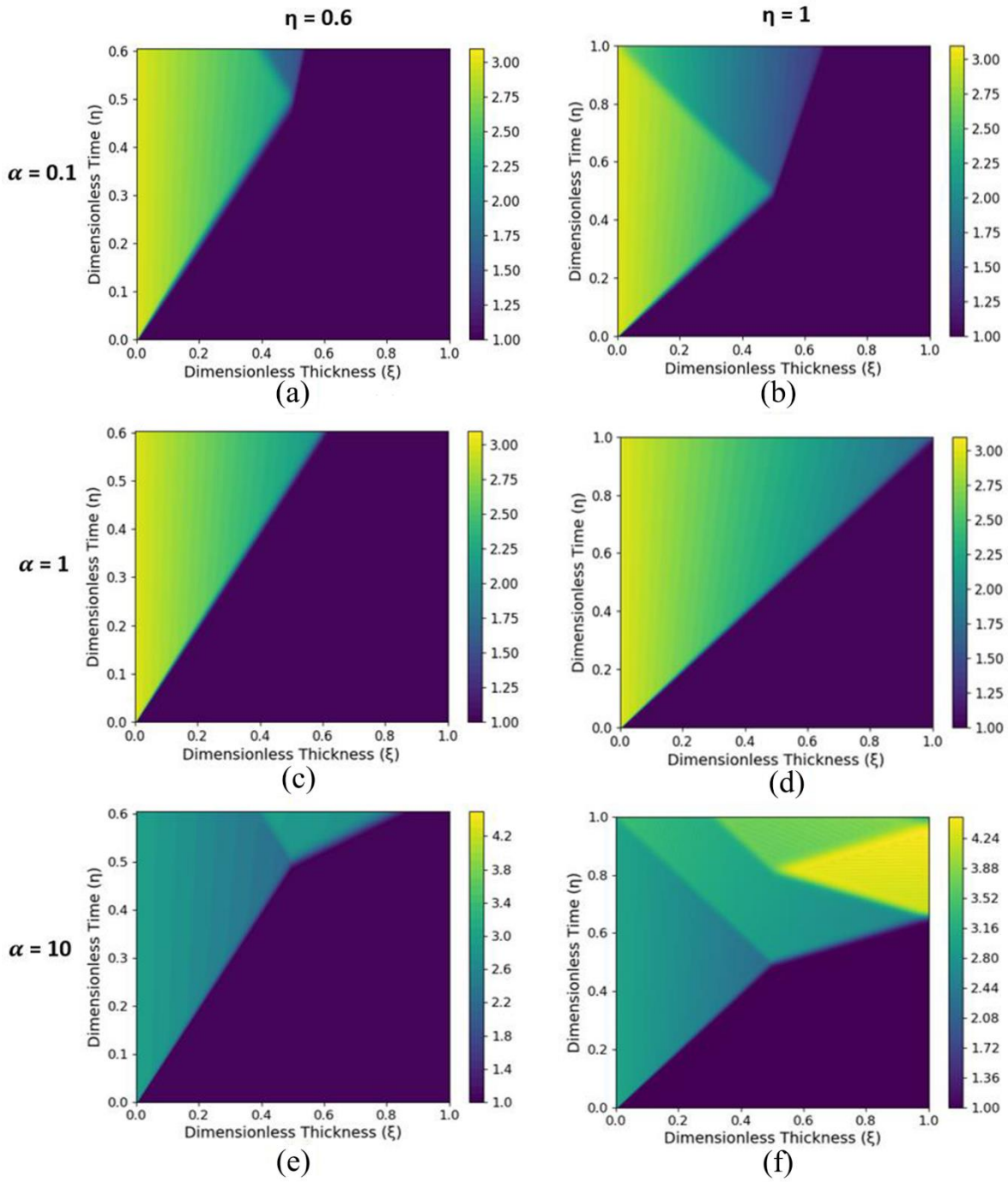

Figure 13. Temperature contours across composite layer from η=0 to η=1 for different thermal diffusivity, (a-b) α=0.1, (c-d) α=1, and (e-f) α=10

The temperature contours across the composite layer from η=0−1 are plotted and shown in Figure 13 for different α. The propagation slowness is noted in Figure 13(a) due to low thermal diffusivity in the substrate. At η=1, the thermal wave reached only the distance ξ≈0.65. Whereas in the case of α=10, higher thermal diffusivity of the substrate thermal wave arrives ξ=1 at η≈0.65 and η=1 the sub-collision occurs in the substrate side as shown in Figure 13(f). The reverse propagation of the thermal wave from the right side of the boundary is faster than the left boundary, and it creates sub-collisions with an increase in temperature θ=4.4 more significant than the applied temperature θ=3. The high-temperature zone occurs at the substrate side after η=0.65.

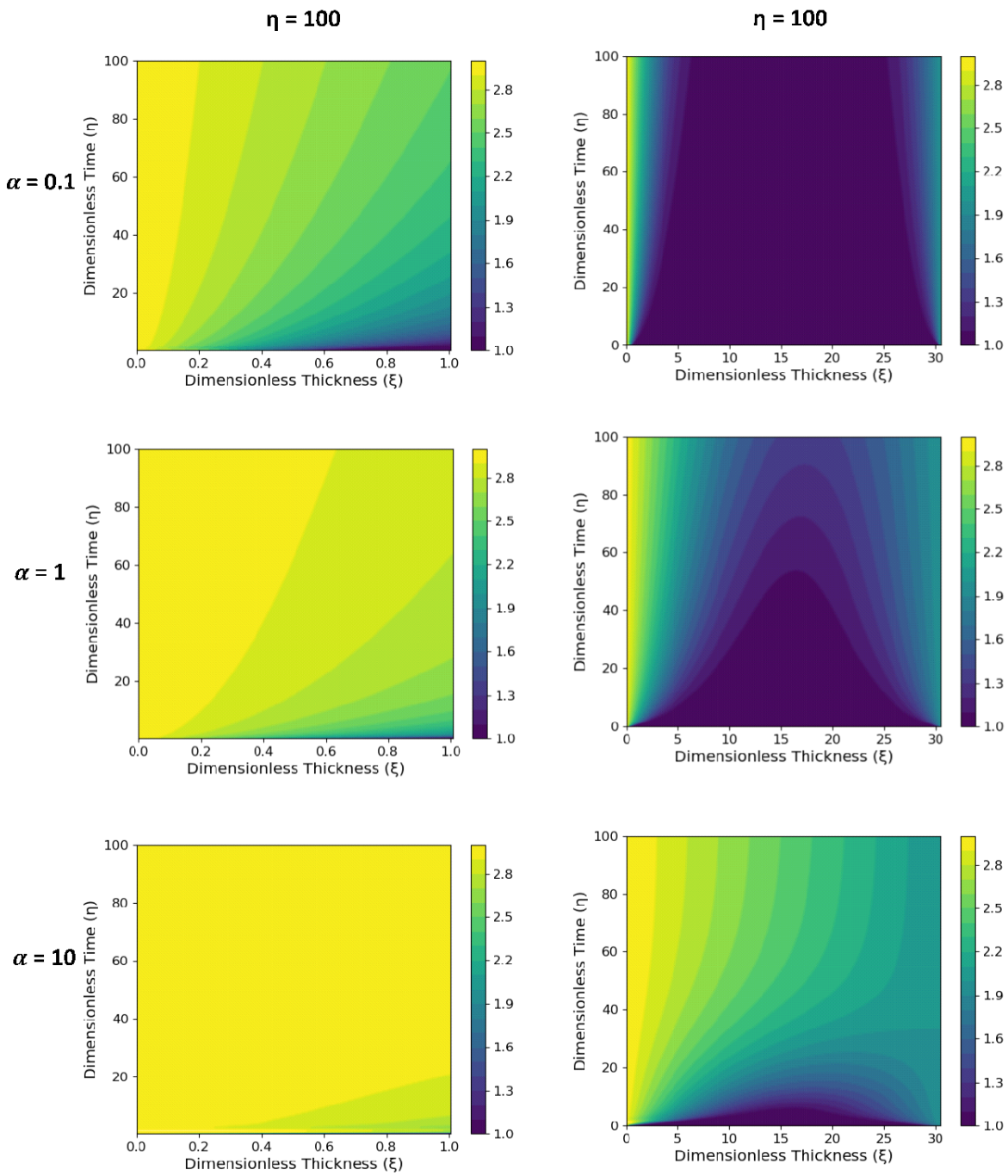

Figure 14. Temperature contours across the composite layer, for ξ=1 and the entire length of the substrate ξ=30.5, at η=100 for different thermal diffusivity α=0.1, α=1 and α=10.

In addition, the temperature contours across the composite layer, for ξ=1 and the entire length of the substrate ξ=30.5, for η=100 with different thermal diffusivity α=0.1, α=1 and α=10 are shown in Figure 14. It is noted that the high-temperature zone occurs near the boundary when α=0.1, throughout the layer when α=10, and is diffused through the layers when α=0.1.

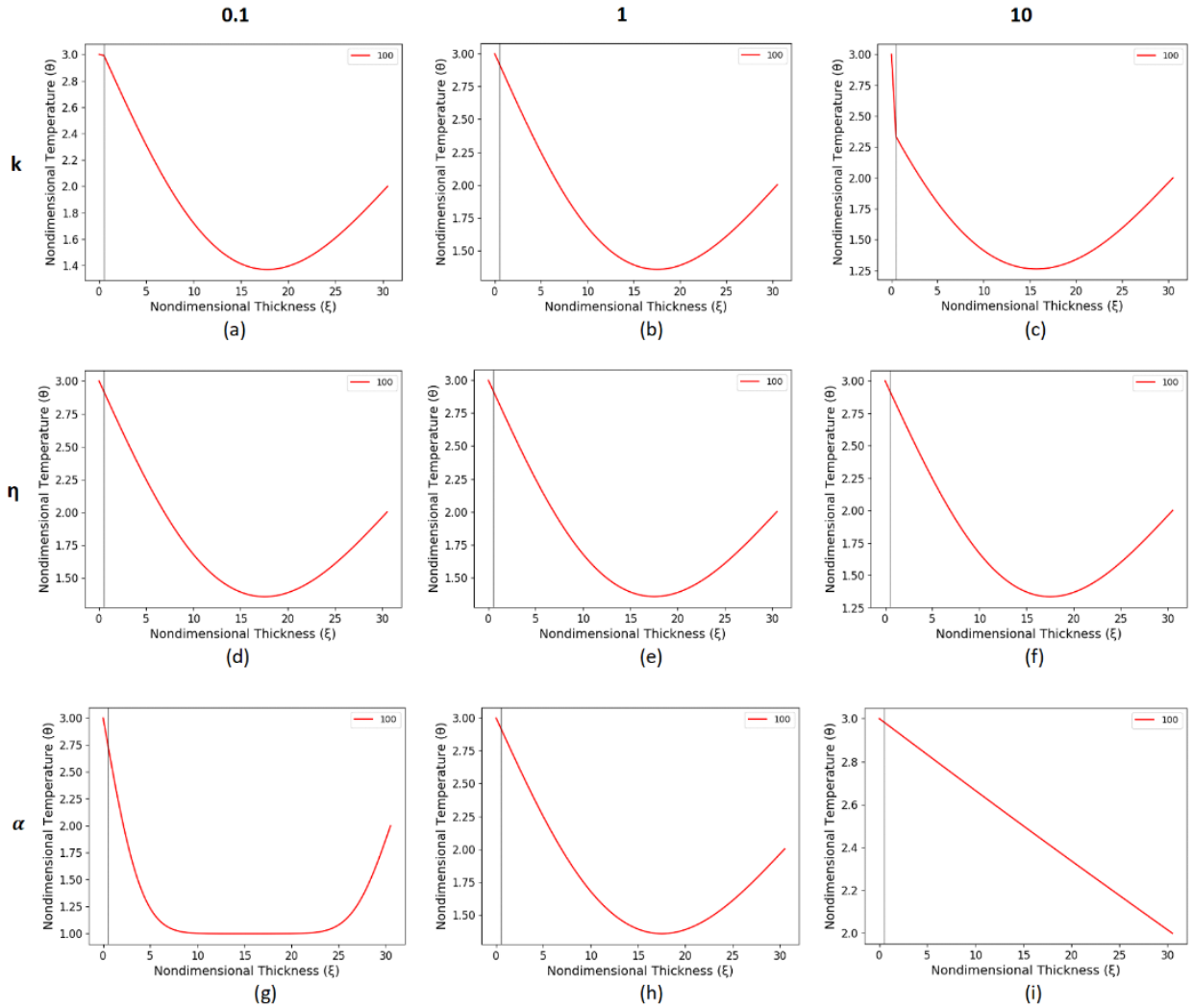

Figure 15. Temperature variation across composite layer for the full length of the substrate at η=100 for different k, τ, and α

Figure 15 shows the temperature variation across the composite layer at η=100. The interface temperature is higher, $\theta \approx 3$, for k=0.1 as demonstrated in Figure 15(a), varies linearly across the coating side and follows parabolic across the substrate side. Figure 15(b) and (c) shows that the interface temperature decreases when k increases and is still in transient condition. Figure 15(d) to (f) reveals that the change in relaxation time never affects the temperature variation across macro layers and still moves towards a steady state. However, Figure 15(g) to (i) shows that the thermal diffusivity increases the interface temperature and reaches a steady state at η=100.

6.0 CONCLUSION

The finite element model is developed to numerically analyze the non-Fourier heat conduction in thin composite layers under asymmetrical boundary conditions. In the thick layer, the thermal wave propagates with finite speed and follows the Fourier heat conduction mode. In contrast, the thermal wave propagates in a thin layer with infinite speed, which disappears the Fourier heat conduction mode. Therefore, analyzing the non-Fourier heat conduction in thin layers is essential. Since the thin layer offers a non-Fourier mode of heat conduction, the present model predicts the heat transfer across the interface of the composite layer. The developed model analyzes thermal wave propagation and collisions across the composite layer by executing in Python using Newmark's scheme and the constant average acceleration method. Temperature contours are plotted for different thermal conductivity k, thermal diffusivity α, and relaxation time τ from time η=0−1 as well as η=0−100. In addition, the temperature variations are shown up to steady-state across the entire substrate length. Through simulations, the following significant finding came out:

1) The temperature increases after the collision at time η>0.5 for k=0.1 and reduces when k=10.
2) The temperature of all the elements on the coating side reaches a high temperature for k=0.1, and the high temperature remains nearer to the boundary for k=10.
3) The thermal wave propagates faster in the substrate, increasing temperature after the first collision at the interface for τ=0.1 and decreasing in temperature after collision with slower propagation in the substrate for τ=10.

4) The thermal wave propagates slower in the substrate, decreasing temperature after the first collision at the interface for α=0.1 and increasing in temperature after collision with faster propagation in the substrate for α=10.

5) The sub-collisions have occurred on the substrate side with a more significant increase in temperature about θ=4.4 for τ=10.

Findings from the present simulations can be used for better heat conduction thin layers applications like thermal barrier coating, condenser, and heat exchangers. The thermal barrier coating applied on the gas turbine becomes ineffective for different circumstances discussed in the present work. The current model provides effective heat conduction across thin composite layers for different thermal conductivity, relaxation time, and thermal diffusivity.

7.0 REFERENCES

[1] C. Cattaneo, "Sur une forme de l'equation de la chaleur eliminant la paradoxe d'une propagation instantantee," *Comptes Rendus de l'Académie des Sciences*, vol. 247, pp. 431–433, 1958.

[2] P. Vernotte, "Les paradoxes de la theorie continue de l'equation de la chaleur," *Comptes Rendus de l'Académie des Sciences*, vol. 246, pp. 3154–3155, 1958.

[3] M. J. Maurer and H. A. Thompson, "Non-Fourier effects at high heat flux," *Journal of Heat and Mass Transfer*, vol. 95, no. 2, pp. 284–286, 1973.

[4] M. N. Özişik and B. Vick, "Propagation and reflection of thermal waves in a finite medium," *International Journal of Heat and Mass Transfer*, vol. 27, no. 10, pp. 1845–1854, 1984.

[5] K. E. Goodson and M. I. Flik, "Electron and phonon thermal conduction in epitaxial high-Tc superconducting films," *Journal of Heat and Mass Transfer*, vol. 115, no. 1, pp. 17–25, 1993.

[6] M. N. O¨zis¸ik and D. Y. Tzou, "On the wave theory in heat conduction," *Journal of Heat and Mass Transfer*, vol. 116, no. 3, pp. 526–535, 1994.

[7] D. Y. Tzou, *Macro- to Microscale Heat Transfer – The Langging Behaviour*, 2nd Eds., John Wiley & Sons Ltd, 2015.

[8] X. Xu, C. P. Grigoropoulos, and R. E. Russo, "Transient temperature during pulsed excimer laser heating of thin polysilicon films obtained by optical reflectivity measurement," *Journal of Heat and Mass Transfer*, vol. 117, no. 1, pp. 17–24, 1995.

[9] Z. M. Tan and W. J. Yang, "Non-Fourier heat conduction in a thin film subjected to a sudden temperature change on two sides," *Journal of Non-Equilibrium Thermodynamics*, vol. 22, no. 1, p. 75, 1997.

[10] Z. M. Tan and W. J. Yang, "Heat transfer during asymmetrical collision of thermal waves in a thin film," *International Journal of Heat and Mass Transfer*, vol. 40, no. 17, pp. 3999–4006, 1997.

[11] L. Wang, "Solution structure of hyperbolic heat-conduction equation," *International Journal of Heat and Mass Transfer*, vol. 43, no. 3, pp. 365–373, 2000.

[12] T. K. Cheung, B. A. Blake, and T. T. Lam, "Heating of finite slabs subjected to laser pulse irradiation and convective cooling," *Journal of Thermophysics and Heat Transfer*, vol. 21, no. 2, pp. 323–329, 2007.

[13] L. Wang, X. Zhou, and X. Wei, *Heat Conduction: Mathematical Models and Analytical Solutions*. 1st Ed., Springer Berlin, Heidelberg, 2007.

[14] A. Moosaie, "Non-Fourier heat conduction in a finite medium with insulated boundaries and arbitrary initial conditions," *International Communications in Heat and Mass Transfer*, vol. 35, no. 1, pp. 103–111, 2008.

[15] M. Lewandowska and L. Malinowski, "An analytical solution of the hyperbolic heat conduction equation for the case of a finite medium symmetrically heated on both sides," *International Communications in Heat and Mass Transfer*, vol. 33, no. 1, pp. 61–69, 2006.

[16] L. A. Peterson, T. K. Cheung, T. T. Lam, and B. A. Blake, "Heat conduction in two-dimensional slabs subjected to spatially decaying laser pulses," *Journal of Thermophysics and Heat Transfer*, vol. 23, no. 1, pp. 18–27, 2009.

[17] T. T. Lam and E. Fong, "Heat diffusion vs. wave propagation in solids subjected to exponentially-decaying heat source: Analytical solution," *International Journal of Thermal Sciences*, vol. 50, no. 11, pp. 2104–2116, 2011.

[18] E. Fong and T. T. Lam, "Asymmetrical collision of thermal waves in thin films: An analytical solution," *International Journal of Thermal Sciences*, vol. 77, pp. 55–65, 2014.

[19] K. Mitra, S. Kumar, A. Vedevarz, and M. K. Moallemi, "Experimental evidence of hyperbolic heat conduction in processed meat," *Journal of Heat and Mass Transfer*, vol. 117, no. 3, pp. 568–573, 1995.

[20] W. Kaminski, "Hyperbolic heat conduction equation for materials with a nonhomogeneous inner structure," *Journal of Heat and Mass Transfer*, vol. 112, no. 3, pp. 555–560, 1990.

[21] W. Roetzel, N. Putra, and S. K. Das, "Experiment and analysis for non-Fourier conduction in materials with non-homogeneous inner structure," *International Journal of Thermal Sciences*, vol. 42, no. 6, pp. 541–552, 2003.

[22] A. L. Koay, S. H. Pulko, and A. J. Wilkinson, "Reverse time TLM modeling of thermal problems described by the hyperbolic heat conduction equation," *Numerical Heat Transfer, Part B: Fundamentals*, vol. 44, no. 4, pp. 347–363, 2003.

[23] S. Torii and W.-J. Yang, "Heat transfer mechanisms in thin film with laser heat source," *International Journal of Heat and Mass Transfer*, vol. 48, no. 3, pp. 537–544, 2005.

[24] W.-B. Lor and H.-S. Chu, "Hyperbolic heat conduction in thin-film high Tc superconductors with interface thermal resistance," *Cryogenics*, vol. 39, no. 9, pp. 739–750, 1999.

[25] W.-B. Lor and H.-S. Chu, "Effect of interface thermal resistance on heat transfer in a composite medium using the thermal wave model," *International Journal of Heat and Mass Transfer*, vol. 43, no. 5, pp. 653–663, 2000.

[26] H.-T. Chen and K.-C. Liu, "Study of hyperbolic heat conduction problem in the film and substrate composite with the interface resistance," *Japanese Journal of Applied Physics*, vol. 41, no. 10, pp. 6267–6275, 2002.

[27] J. Li, P. Cheng, G. P. Peterson, and J. Z. Xu, "Rapid transient heat conduction in multilayer materials with pulsed heating boundary," *Numerical Heat Transfer Applications Part A*, vol. 47, no. 7, pp. 633–652, 2005.

[28] S. Akwaboa, P. Mensah, E. Beyazouglu, and R. Diwan, "Thermal modeling and analysis of a thermal barrier coating structure using non-Fourier heat conduction," *Journal of Heat and Mass Transfer*, vol. 134, no. 11, 2012.

[29] R. Yuvaraj and D. Senthil Kumar, "Numerical simulation of thermal wave propagation and collision in thin film using finite element solution," *Journal of Thermal Analysis and Calorimetry*, vol. 142, no. 6, pp. 2351–2369, 2020.

[30] M. Mozafarifard, S. M. Mortazavinejad, and D. Toghraie, "Numerical simulation of fractional non-Fourier heat transfer in thin metal films under short-pulse laser," *International Communications in Heat and Mass Transfer*, vol. 115, p. 104607, 2020.

[31] Y. Liu, L. Li, and Y. Zhang, "Numerical simulation of non-Fourier heat conduction in fins by lattice Boltzmann method," *Applied Thermal Engineering*, vol. 166, p. 114670, 2020.

[32] R.-Y. Dong, Y. Dong, and A. Sellitto, "An analogy analysis between one-dimensional non-Fourier heat conduction and non-Newtonian flow in nanosystems," *International Journal of Heat and Mass Transfer*, vol. 164, p. 120519, 2021.

[33] A. Khosravirad and M. B. Ayani, "Comparative analysis of thermal damage to laser-irradiated breast tumor based on Fourier conduction and non-Fourier heat conduction models: A numerical study," *International Communications in Heat and Mass Transfer*, vol. 145, p. 106837, 2023.

[34] J. S. Hu, B. L. Wang, H. Hirakata, and K. F. Wang, "Thermal shock fracture analysis of auxetic honeycomb layer based on non-Fourier heat conduction," *Engineering Structures*, vol. 279, p. 115581, 2023.

[35] J. N. Reddy, *An Introduction to the Finite Element Method*, 3rd ed., McGraw-Hill Education, 2005.